



**HAL**  
open science

## Acoustic impacts of geometric approximation at the level of velum and epiglottis on French vowels

Ioannis K Douros, Pierre-André Vuissoz, Yves Laprie

► **To cite this version:**

Ioannis K Douros, Pierre-André Vuissoz, Yves Laprie. Acoustic impacts of geometric approximation at the level of velum and epiglottis on French vowels. ICPHS 2019 - International Congress of Phonetic Sciences, Aug 2019, Melbourne, Australia. hal-02180566

**HAL Id: hal-02180566**

**<https://inria.hal.science/hal-02180566>**

Submitted on 11 Jul 2019

**HAL** is a multi-disciplinary open access archive for the deposit and dissemination of scientific research documents, whether they are published or not. The documents may come from teaching and research institutions in France or abroad, or from public or private research centers.

L'archive ouverte pluridisciplinaire **HAL**, est destinée au dépôt et à la diffusion de documents scientifiques de niveau recherche, publiés ou non, émanant des établissements d'enseignement et de recherche français ou étrangers, des laboratoires publics ou privés.

# ACOUSTIC IMPACTS OF GEOMETRIC APPROXIMATION AT THE LEVEL OF VELUM AND EPIGLOTTIS ON FRENCH VOWELS

Ioannis K. Douros<sup>1,2</sup>, Pierre-André Vuissoz<sup>2</sup>, Yves Laprie<sup>1</sup>

<sup>1</sup>Université de Lorraine, CNRS, Inria, LORIA, F-54000 Nancy, France,

<sup>2</sup>Université de Lorraine, INSERM U1254, IADI, F-54000 Nancy, France,  
ioannis.douros@loria.fr, pa.vuissoz@chru-nancy.fr, yves.laprie@loria.fr

## ABSTRACT

In this work we study the effect of the velum and epiglottis on speech production of five French vowels. Our purpose is to examine whether it is possible to simplify the geometry of the vocal tract in the framework of articulatory synthesis to achieve a simpler geometric description without changing the acoustic properties. In the present study, we use MRI to acquire the 3D shape of the vocal tract with simultaneous recording of the speech signal. The geometric two-dimensional shape derived from these data was used as an input of numerical acoustic simulations. The geometrical shape was edited at the level of epiglottis and velum (with or without epiglottis, with or without a constant wall approximation at velum) and the spectra obtained via numerical acoustic simulations were compared with those obtained from audio recordings. This allows the impact of these articulators and geometrical simplifications to be assessed.

**Keywords:** velum, epiglottis, speech production, acoustic simulation, French vowels

## 1. INTRODUCTION

Geometric modeling of the vocal tract is used in particular to produce input data for articulatory synthesis [2]. One of the challenges is to obtain a concise description and to remove geometric details that do not change the acoustic parameters significantly, from a perceptual point of view. Those simplifications could lead to a reduction of the number of parameters used to describe the vocal tract geometry, and consequently make the calculation simpler.

In general, more attention is paid to the jaw, tongue, lips and larynx, compared to the velum and epiglottis. The velum is indirectly taken into account more for representing the opening of the velopharyngeal port than for its impact on the oral cavity.

Concerning the epiglottis, its position depends on the size of the pharyngeal cavity, and thus on the

tongue position. For a vowel with a large back cavity (as in /i/), the epiglottis stays apart from the back of the tongue. On the other hand, when the back cavity is more constricted (as for /a/), the epiglottis is sometimes pressed against the back of the tongue.

Our approach to geometric modeling of the vocal tract is based on an articulatory model that independently controls each of the articulators. The first articulator is the mandible (which corresponds to the opening of the jaw) because it influences the tongue and the lips. Two parameters are sufficient to control the opening of the jaw with good precision. The tongue is the articulator that achieves the greatest number of articulation places, and its description must be fine enough to reach a precise position and shape. For this reason, (unlike the Maeda model [10]), we use between 6 and 10 deformation factors. The influence of the jaw is taken into account to determine the influence of the tongue and lips.

The epiglottis is actually a cartilage, and therefore the influence of other articulators that interact with the epiglottis, i.e. the mandible, tongue, and larynx, is decisive. Hence, their contribution through linear regression factors is more important than its intrinsic deformation factors. Once the midsagittal shape is calculated, it is necessary to find all the resonating cavities, their area functions and the global topology to run the acoustic simulation [6]. Geometrical simplifications would allow faster simulations and avoid changes of the global topology when a small cavity appears.

The objective of this work is to investigate the impact of geometric simplifications in order to better understand those that can be made without removing important acoustic cues. Unlike Arnela's work [1], which treats the vocal tract as a whole by transforming it into a piece-wise elliptical and then cylindrical tube, we treat the articulators separately because articulatory synthesis requires that each of them be controlled independently of each other.

We used MRI data of the vocal tract with simul-

taneous speech recordings of five French vowels to study the articulators' effects. The real speech signal was used as a reference. We edited the images to remove the velum and the epiglottis and then used acoustic simulations to see how the transfer function of the vocal tract was affected, and, therefore, what the role is of these two articulators in phonation.

## 2. MATERIALS AND METHODS

### 2.1. Data

For the purpose of this study, we used an MRI data part of a study approved by an ethics committee and the subject gave written informed consent (ClinicalTrials.gov identifier: NCT02887053). The subject retained for the data acquisition is a healthy male French native speaker at the age of 32, without any reported speaking or hearing problems.

The MRI data (same as described in [5]) was acquired on a Siemens Prisma 3T scanner (Siemens, Erlangen, Germany). We used the 3-dimensional cartesian vibe sequence ( $TR = 3.57\text{ ms}$ ,  $TE = 1.43$ ,  $FOV = 22 \times 20\text{ mm}$ ,  $flip\ angle = 9\ degrees$ ) for the acquisition. To acquire the speech signal, we used FOMRI III (Optoacoustics, Or Yehuda, Israel) fiber optic microphone. Since the audio recordings were made at the same time as the MRI acquisition, we used FASST toolbox [12] to denoise the speech signal using the denoising algorithm proposed in [11]. Despite the improvement of the signal quality for-mant frequencies cannot be easily determined, especially above 2500 Hz. Values of Table 1 are thus given as an indication, especially those above 2000 Hz, and not as a reference.

### 2.2. MRI data processing

The process of MRI data is mainly divided in two steps: 1) pre-process the data to make some corrections regarding the orientation of the 3D images axis and 2) segment the vocal tract.

To make adjustments to the axis of the 3D images we used 3DSlicer software [8] (<http://www.slicer.org>). Among its several functions, like visualizing and processing various types of medical images such as MRI and CT, 3DSlicer can be used to resample the images using several kinds of interpolation techniques like linear or Lanczos.

For the image segmentation tasks, we used ITK-SNAP software [17]. It is a software designed to segment medical images and offers tools and algorithms both for 2D and 3D image segmentation. For example, it provides region competition and

geodesic active contours algorithms for automatic segmentation [3, 18]. As far as manual segmentation is concerned, it offers polygon-based tools and various types of paint brushes in order to specify the segmented region.

### 2.3. Acoustic simulations

For the purposes of our experiments, we used k-wave toolbox for MATLAB [15] to simulate how the acoustic wave propagates through the vocal tract until it reaches the lips. The applications of k-wave toolbox range from acoustic [14] and ultrasound wave propagation [16], [9] to photoacoustic tomography [13].

Although there are various popular methods for acoustic wave propagation, like finite differences, finite elements and boundary element methods, they generally take a significant amount of time since they require a small time step and a lot of grid points per wavelength. k-wave solves these issues by interpolating a Fourier series through all of the grid points to get an estimation of the gradient. This way, the computations are faster since they require less grid points and employ Fast Fourier Transform (FFT) to make the calculations. An issue that arises is that as the wave reaches the grid boundaries, it keeps propagating by entering from the opposite site. To prevent this, k-wave implements an absorbing boundary condition called Perfect Match Layer (PML).

## 3. EXPERIMENTS

The experiment consisted of two parts: 1) image processing and 2) acoustic simulations.

### 3.1. Image processing

In this experiment we used five vowels of the French language, /a, œ, i, o, y/. First, we used 3DSlicer software to correct the axis orientation of the 3D images since there was a small angular offset of about  $-6$  degrees in the sagittal field. We used Lanczos interpolation to resample the image with the Lanczos filter parameter chosen as  $a = 4$ .

When then employed the ITK-SNAP software for semi-automatic segmentation of the vocal tract 3D volume.

The Nearest Neighbourhood algorithm was used to create the probabilistic map to use for the automatic segmentation of the vocal tract. We used two classes and 10000 points for consideration as the nearest points for class categorization for the creation of the probabilistic map. Then an active con-

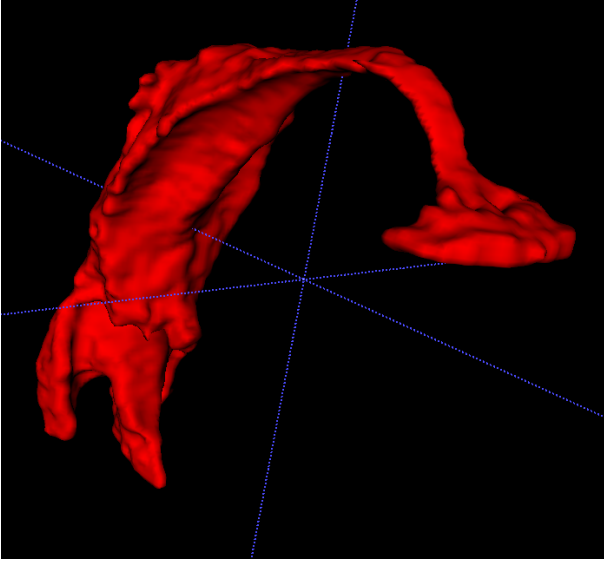


**Figure 1:** 3D volume of /i/ vowel tour algorithm was applied and the vocal tract mesh generated (Figure 1).

### 3.2. Editing of the vocal tract geometry

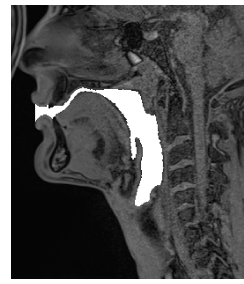
Since the impact of the 3rd dimension to the acoustics of the vowels is not very significant [7, 5], we extracted the mid-sagittal slices from the 3D shapes to further process and use for our study. We used the 3D shape as a guide to correct segmentation errors in the mid-sagittal slices (especially in the region of velum and epiglottis) caused by blurring due to image interpolation.

For every mid-sagittal slice, three more segmentation versions were created by processing the segmented images (4 images per vowel in total with the original). In the first version we edited the vocal tract geometry to withdraw the epiglottis, in the second we used a constant wall approximation at velum (by withdrawing the velum extremity) and in the third version we combined the previously described simplifications (Figure 2). These three versions of every vowel along with the original were the data used in the simulations.

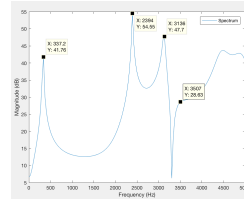
Finally we used meshlab [4] to smooth every mesh by applying Laplacian smoothing filter with step 3. For every vowel, about 5 hours of processing was required, with the biggest amount of time spent on the manual segmentation step.

### 3.3. Acoustic simulations

The simulation code that we used was built in MATLAB environment using k-wave toolbox. The data used as an input are in the form of a 3D surface mesh with sagittal width 1.2mm. We transformed



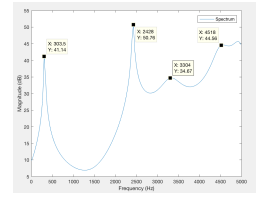
2D segmentation of /i/ vowel with full vocal tract



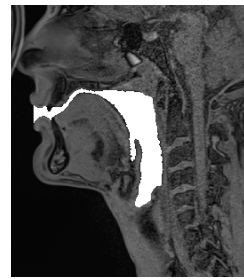
Spectrum of /i/ vowel with full vocal tract



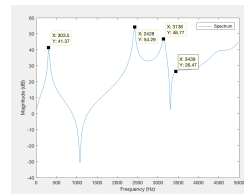
2D segmentation of /i/ vowel without epiglottis



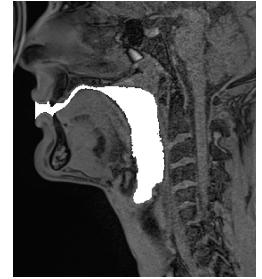
Spectrum of /i/ vowel without epiglottis



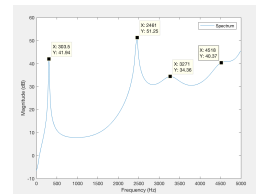
2D segmentation of /i/ vowel without velum



Spectrum of /i/ vowel without velum



2D segmentation of /i/ vowel without epiglottis and velum



Spectrum of /i/ vowel without epiglottis and velum

**Figure 2:** The four versions of /i/ phoneme (original, without epiglottis, without velum, without velum and epiglottis) with the corresponding spectrums below them

the surface mesh into a volumetric representation using voxels and we took the projection of the voxel-based geometry to a 2D plane parallel to the sagittal field. Finally we ran the simulations.

A challenge that we faced was specifying the parameters of the simulation so that there would be a balance between the stability of the simulation, a

good approximation of the realistic conditions and a sufficient duration of simulated signal. In our case, the computational grid has a size of  $128 \times 128$  (coronal  $\times$  axial) with grid spacing  $d_x = d_y = 1mm$ . A PML layer of 10 grid points was added at the boundaries of every side to solve the issue of circular wave propagation that happens when simulating with k-wave, the problem that was mentioned in the method section. We manually select the source position for every vowel to correspond to the position of the vocal folds. As a source, we used a disc of 5 grid point radius that emits a *delta* pulse of pressure (spreading equally in all directions) and  $1Pa$  amplitude. The medium properties inside the vocal tract were  $c_{in} = 350m/s, d_{in} = 1kg/m^3$  and the properties outside were  $c_{out} = 1000m/s, d_{out} = 1000kg/m^3$ , where  $c_{in}, c_{out}$  are the speed, and  $d_{in}, d_{out}$  are the densities inside and outside the vocal tract respectively. We simulated the signal for  $30ms$ , with a time of  $3 * 10^{-8}$ , resulting in 1000001 signal samples. The pressure signal was recorded with a sensor placed at the end of the vocal tract and the maximum allowed frequency of the grid was  $175KHz$ . Every simulation requires on average 3 hours and 20 minutes.

Finally we computed the transfer function of every vocal tract and computed the peaks that appear in the frequency domain to compare them with the formants of the original audio signal (Table 1).

#### 4. DISCUSSION

The first remark concerns the values of the formant frequencies of the normal vocal tract without simplifications. The lying position and noise in the MRI machine largely explain the deviations from the expected values for these vowels of a male speaker.

The second remark, which is illustrated by Figure 2 is that the original geometry with the small cavity between the epiglottis and tongue root gives rise to a zero in the spectrum. This is all the more pronounced since the epiglottis is well separated from the tongue. In the case of the vowel /i/, it is also noted that a zero appears in the region of F3-F4.

Regarding simplifications, it should be noted in Table 1 that they do not have a very significant impact on the first formant. For F2, the velum simplification has a more pronounced effect. The changes at the velum have an impact on the constriction between the front and back cavities of the vocal tract. This mainly affects F2 which is more sensitive to the length of the cavities.

As can be seen on the spectra of numerical simulations, the impact of the epiglottis corresponds to the appearance of a small cavity that adds zeros in

**Table 1:** speech signal / simulations with full vocal tract / simulations without epiglottis (no\_epig) / simulations without velum (no\_vel) / simulations without epiglottis and velum (no\_epig\_vel) formants computation in Hertz for the five vowels.

	F1	F2	F3
/a/ - speech signal	689	1296	2604
/a/ - full vocal tract	674	1349	3169
/a/ - no_epig	641	1315	3405
/a/ - no_vel	674	1787	2933
/a/ - no_epig_vel	674	1753	2832
/œ - speech signal	443	1335	2436
/œ - full vocal tract	416	1444	2471
/œ - no_epig	417	1444	2499
/œ - no_vel	389	1527	2360
/œ - no_epig_vel	389	1527	2332
/i/ - speech signal	380	2306	3193
/i/ - full vocal tract	337	2394	3136
/i/ - no_epig	304	2428	3304
/i/ - no_vel	304	2428	3136
/i/ - no_epig_vel	304	2461	3271
/o/ - speech signal	430	732	2619
/o/ - full vocal tract	404	900	2001
/o/ - no_epig	404	900	2728
/o/ - no_vel	404	1012	2422
/o/ - no_epig_vel	404	990	2391
/y/ - speech signal	336	1854	2228
/y/ - full vocal tract	281	1798	2192
/y/ - no_epig	253	1798	2220
/y/ - no_vel	251	1826	2192
/y/ - no_epig_vel	253	1826	2164

the spectrum, essentially at high frequency since this cavity is small. Nevertheless, the impact of this cavity is far from being negligible above  $2500Hz$  when the epiglottis is well separated from the tongue (thus not for /a/) because the zero appears in the region of F3 and/or F4. Further work will focus on the development of simplification control algorithms to ensure that they have as little impact as possible on the formants.

#### 5. ACKNOWLEDGEMENT

This work was financed by Lorraine Université d'Excellence (LUE) grant and ANR ArtSpeech.

#### 6. REFERENCES

- [1] Arnela, M., Dabbaghchian, S., Blandin, R., Guasch, O., Engwall, O., Van Hirtum, A., Pelorson, X. 2016. Influence of vocal tract geometry simplifications on the numerical simulation of vowel sounds. *The Journal of the Acoustical Society of America* 140(3), 1707–1718.

- [2] Birkholz, P., Jackel, D. Aug 2003. A three-dimensional model of the vocal tract for speech synthesis. *15th International Congress of Phonetic Sciences - ICPhS'2003, Barcelona, Spain* 2597–2600.
- [3] Caselles, V., Kimmel, R., Sapiro, G. 1997. Geodesic active contours. *International journal of computer vision* 22(1), 61–79.
- [4] Cignoni, P., Callieri, M., Corsini, M., Dellepiane, M., Ganovelli, F., Ranzuglia, G. 2008. Meshlab: an open-source mesh processing tool. *Eurographics Italian Chapter Conference* volume 2008 129–136.
- [5] Douros, I. K., Vuissoz, P.-A., Laprie, Y. 2019. Comparison between 2d and 3d models for speech production: a study of french vowels. *International Congress on Phonetic Sciences, Melbourne, Australia*.
- [6] Elie, B., Laprie, Y. Sept. 2016. Extension of the single-matrix formulation of the vocal tract: consideration of bilateral channels and connection of self-oscillating models of the vocal folds with a glottal chink. *Speech Communication* 82, 85–96.
- [7] Ericsson, C. 2007. Detail in vowel area functions. *Proc of the 16<sup>th</sup> ICPhS Saarbrücken, Germany*. 513–516.
- [8] Fedorov, A., Beichel, R., Kalpathy-Cramer, J., Finet, J., Fillion-Robin, J.-C., Pujol, S., Bauer, C., Jennings, D., Fennessy, F., Sonka, M., others, 2012. 3d slicer as an image computing platform for the quantitative imaging network. *Magnetic resonance imaging* 30(9), 1323–1341.
- [9] Jaros, J., Treeby, B. E., Rendell, A. P. 2012. Use of multiple gpus on shared memory multiprocessors for ultrasound propagation simulations. *Proceedings of the Tenth Australasian Symposium on Parallel and Distributed Computing-Volume 127*. Australian Computer Society, Inc. 43–52.
- [10] Maeda, S. 1990. Compensatory articulation during speech: Evidence from the analysis and synthesis of vocal-tract shapes using an articulatory model. In: Hardcastle, W., Marchal, A., (eds), *Speech production and speech modelling*. Amsterdam: Kluwer Academic Publisher 131–149.
- [11] Ozerov, A., Vincent, E., Bimbot, F. 2012. A general flexible framework for the handling of prior information in audio source separation. *IEEE Transactions on Audio, Speech, and Language Processing* 20(4), 1118–1133.
- [12] Salaün, Y., Vincent, E., Bertin, N., Souviraà-Labastie, N., Jaureguiberry, X., Tran, D. T., Bimbot, F. 2014. The flexible audio source separation toolbox version 2.0. *ICASSP*.
- [13] Treeby, B. E. 2013. Acoustic attenuation compensation in photoacoustic tomography using time-variant filtering. *Journal of biomedical optics* 18(3), 036008.
- [14] Treeby, B. E., Cox, B. 2010. Modeling power law absorption and dispersion for acoustic propagation using the fractional laplacian. *The Journal of the Acoustical Society of America* 127(5), 2741–2748.
- [15] Treeby, B. E., Cox, B. T. 2010. k-wave: Matlab toolbox for the simulation and reconstruction of photoacoustic wave fields. *Journal of biomedical optics* 15(2), 021314.
- [16] Wise, E. S., Treeby, B. E. 2013. Full-wave nonlinear ultrasound simulation in an axisymmetric coordinate system using the discrete sine and cosine transforms. *Ultrasonics Symposium (IUS), 2013 IEEE International*. IEEE 1374–1377.
- [17] Yushkevich, P. A., Piven, J., Hazlett, H. C., Smith, R. G., Ho, S., Gee, J. C., Gerig, G. 2006. User-guided 3d active contour segmentation of anatomical structures: significantly improved efficiency and reliability. *Neuroimage* 31(3), 1116–1128.
- [18] Zhu, S. C., Yuille, A. 1996. Region competition: Unifying snakes, region growing, and bayes/mdl for multiband image segmentation. *IEEE transactions on pattern analysis and machine intelligence* 18(9), 884–900.